Geophysical Research Letters

Key Points:
- Seafloor massive sulfide deposits can be detected/mapped on a large scale with controlled source electromagnetic methods
- Multidisciplinary geophysical data analysis and local probing lead to a rigorous interpretation of deposit dimensions and resource potential
- Sulfide ore content reduces with depth down to a few tens of meters into the deposit's altered basalt and silica-dominated root

Marine Mineral Exploration With Controlled Source Electromagnetics at the TAG Hydrothermal Field, 26°N Mid-Atlantic Ridge

R. A. S. Gehrmann[1] [ID], L. J. North[2], S. Graber[3], F. Szitkar[3,4], S. Petersen[3], T. A. Minshull[1] [ID], and B. J. Murton[2] [ID]

[1]University of Southampton, Ocean and Earth Sciences, National Oceanography Centre Southampton, Southampton, UK, [2]National Oceanography Centre, Southampton, UK, [3]GEOMAR-Helmholtz Centre for Ocean Research Kiel, Kiel, Germany, [4]Japan Agency for Marine-Earth Science Technology, JAMSTEC, Center for Earthquakes and Tsunami, Yokosuka, Japan

Abstract Seafloor massive sulfide (SMS) deposits are of increasing economic interest in order to satisfy the relentless growth in worldwide metal demand. The Trans-Atlantic Geotraverse (TAG) hydrothermal field at 26°N on the Mid-Atlantic Ridge hosts several such deposits. This study presents new controlled source electromagnetic, bathymetric, and magnetic results from the TAG field. Potential SMS targets were selected based on their surface expressions in high-resolution bathymetric data. High-resolution reduced-to-the-pole magnetic data show negative anomalies beneath and surrounding the SMS deposits, revealing large areas of hydrothermal alteration. Controlled source electromagnetic data, sensitive to the electrical conductivity of SMS mineralization, further reveal a maximum thickness of up to 80 m and conductivities of up to 5 S/m. SMS samples have conductivities of up to a few thousand Siemens per meter, suggesting that remotely inferred conductivities represent an average of metal sulfide ores combined with silicified and altered host basalt that likely dominates at greater depths.

Plain Language Summary Seafloor massive sulfide deposits, formed by high-temperature hydrothermal activity, provide a potential resource for metals including copper, zinc, lead, gold, and silver. Here, we report the results of a geophysical study to estimate the distribution and size of seafloor ore deposits at the Trans-Atlantic Geotraverse hydrothermal field, located south of the Azores, on the Mid-Atlantic Ridge. The Trans-Atlantic Geotraverse field hosts numerous deposits, all but one of which are hydrothermally inactive. Inactive deposits are economically more valuable but difficult to detect. Our solution is a combination of high-resolution seafloor and subseafloor mapping techniques. By focusing on exploration using ship-towed electromagnetic sensing and autonomous underwater vehicle-based mapping and characterization of their magnetic field, we exploit unique signatures identifying these deposits from their surrounding volcanic rock. These data enable us to delineate the extent of the deposits and provide a first estimate of their thickness. We integrate physical and chemical properties of ore and host rock samples, recovered by drilling, into our interpretation in order to estimate the full economic potential of the deposits. Our results reveal a deposit geometry consisting of a sulfide ore body that is mixed with an increasing amount of silica and altered volcanic rocks at depth.

1. Introduction

Seafloor massive sulfide (SMS) deposits are considered a potential resource for economically valuable metals such as copper, zinc, lead, gold, and silver as well as for trace metals necessary for green or new technologies. Increasing global demand and insecure supply on land lead many countries to target the deep sea for future mineral resources (Hannington et al., 2011; Rona, 2003). While active vent fields are dominantly explored using geochemical sensors that search for anomalies in the water column, inactive fields do not exhibit such a prominent signature. Inactive SMS deposits, however, are estimated to contain a larger amount of metal sulfides and are characterized by the absence of high-temperature venting and the commonly associated low pH values: two factors viewed as positive for possible mining operations (Hannington et al., 2011). The assessment of the quality and amount of SMS deposits sufficient for resource calculations requires both
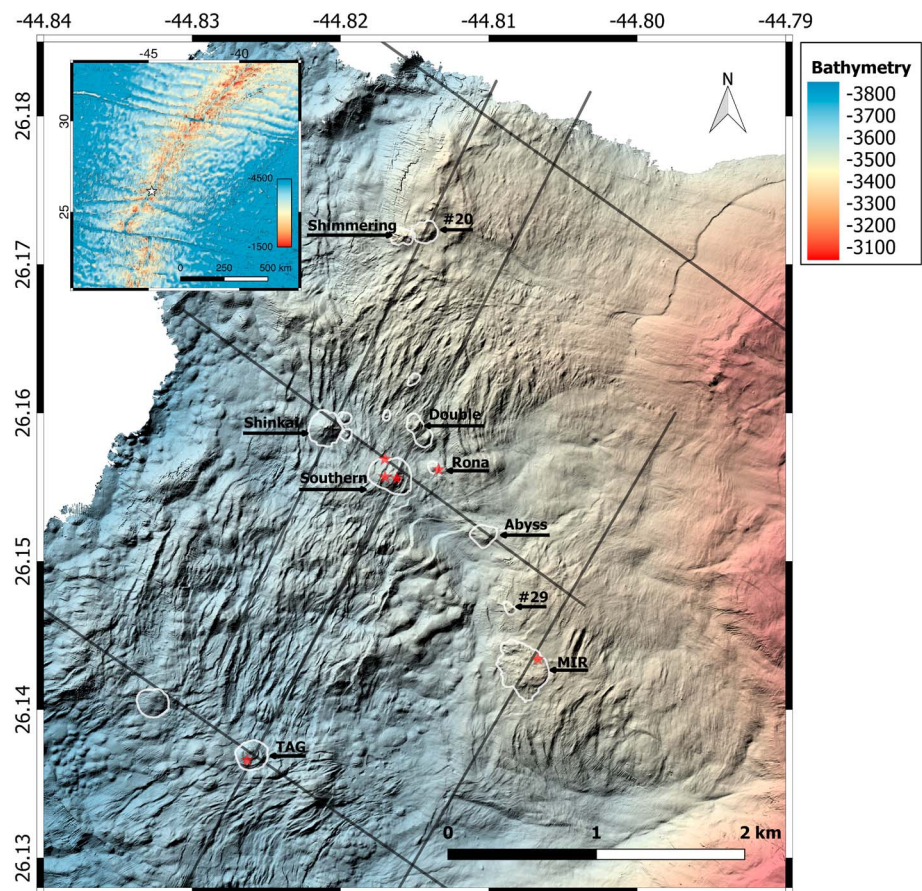
Figure 1. High-resolution (2 m) bathymetry map of the TAG hydrothermal field at the Mid-Atlantic Ridge (white star in overview map): Bathymetry from the autonomous underwater vehicle Abyss survey (Petersen and shipboard scientific party, 2016) overlain by its hill shading (lit from the NNW). White liner mark seafloor massive sulfide targets identified from the bathymetry. The red stars are the location of samples for which physical properties were measured. The neovolcanic zone is about 2 km to the NW of the map. The black lines are the controlled source electromagnetic survey lines. TAG = Trans-Atlantic Geotraverse.

fast and cost-effective remote exploration to evaluate the distribution and size of the deposits and localized drilling to understand the resource potential of any given site.

The Trans-Atlantic Geotraverse (TAG) field (Figure 1), located at 26°08′ N, covering an area of about 5×5 km^2 is the largest and best studied hydrothermal field on the Mid-Atlantic Ridge. It hosts, in addition to the active TAG mound, several inactive SMS deposits. Hydrothermal activity in the area may have started as early as 140 kyr ago (Humphris et al., 1995). Radiometric data indicated that the formation of massive sulfides at the active TAG mound started some 50 to 20 kyr ago with high-temperature pulses every 5–6 kyr (Lalou et al., 1995). The inactive sulfide occurrences comprise the MIR zone, the oldest deposit, to the east of TAG mound, and a number of mounds to the north of TAG mound in an area that was originally called the Alvin zone (Rona et al., 1993). The Alvin zone includes the large Shinkai, Southern, Shimmering, and Double mound (White et al., 1998) as well as a series of smaller sulfide mounds (e.g., Rona mound; Figure 1).

During summer 2016, an international and interdisciplinary survey with two back-to-back cruises was conducted in the TAG hydrothermal field to study the geophysical and geochemical signature of SMS deposits. The survey comprised high-resolution bathymetric mapping and magnetic data acquisition from the autonomous underwater vehicle (AUV) Abyss (GEOMAR) and controlled source electromagnetic (CSEM) experiments among others. Additionally, seafloor coring with the lander-type seafloor drilling rig RD2 (British Geological Survey) and video imaging with the remotely operated vehicle (ROV) HyBis (National Oceanography Centre) were also conducted. Physical and chemical properties of the sulfide sam-

ples and sediment cores were measured shoreside in the lab (Murton et al., 2019). Here, we present results from this work with emphasis on the towed CSEM study regarding SMS detection and size estimation.

The CSEM method is sensitive to contrasts in electrical conductivity. For example, the largest component of an SMS deposits is expected to be precipitated sulfide (e.g., pyrite and iron sulfide) which is a semiconductor. According to drilling results obtained by the Ocean Drilling Program on TAG mound (Herzig et al., 1998; Humphris et al., 1995) and RD2 drilling on the inactive mounds (Lehrmann et al., 2018), the host rock underneath the deposits is likely to comprise less conductive fresh and hydrothermally altered basalts for which conductivity is controlled by electrolytes (salt water) in the pore space. Due to the mound size (up to a few hundreds of meters in diameter) and their potential for significant conductivity contrasts, SMS deposits may be detected with remote electromagnetic methods such as horizontal dipole-dipole arrays (Cairns et al., 1996; Edwards & Chave, 1986; Evans & Everett, 1994). Here, we present new CSEM data acquired over several kilometers with a large footprint of up to a few hundred meters interpreted with complementary interdisciplinary data to solve the problem of reliable resource assessment for SMS deposits.

## 2. Methods

2.1. Controlled Source Electromagnetics

The CSEM system presented here is comprised of the Deep-towed Active Source Instrument (DASI; Sinha et al., 1990) and two three-axis electric field receivers (Vulcan; Constable et al., 2016) towed at 350 and 505 m behind DASI. The DASI-Vulcan array was towed between 50 and 150 m above the seafloor at a constant speed of 1.852 km/hr. An alternating square waveform with a current amplitude of about 90 A and a base frequency of 1 Hz was transmitted through a 50-m-long bipole antenna. Six-multikilometer-long survey profiles were acquired across the active TAG mound and several inactive SMS deposits (Figure 1).

Data processing comprised a fast-Fourier transformation of 1-s-long time windows, deconvolution with the transmitter signal, and stacking of 30-s-long windows (Text S1 in the supporting information; Myer et al., 2011). Including navigational information, the amplitude of the data for frequencies of 1–5 Hz was evaluated along each profile. There is no direct way to interpret CSEM data for a heterogeneous seafloor conductivity model. Instead, the conductivity model below the seafloor must be inferred with inversion algorithms. Here, we implement a two-dimensional (2-D) inversion (MARE2DEM; Key, 2016): a linearized scheme based on Occam's razor, searching for the simplest model that can explain the data (Text S1; Constable et al., 1987). The final conductivity model favors gradual changes and only includes abrupt changes between model cells if the data sensitivity is high enough. Generally, data sensitivity reduces with increasing depth but also depends on the assumed data error, which we have assessed with a detailed error analysis using forward modeling that includes uncertainties caused by navigation over rough terrain (Text S1). Also, an ambiguity arises between a thicker, less conductive body and a thinner, more conductive body. In fact, the conductivity-thickness product, the conductance, can often be better resolved (e.g., Edwards, 1997) than individual parameters alone. Despite this ambiguity, the inferred thickness does not deviate by more than a few tens of meters from the actual thickness because the model is constrained by two receivers at different offsets to the source and three different frequencies, allowing the dipole-dipole system to be sensitive to the less conductive material below the sulfide ore body.

For each profile, the conductance is calculated as the integrated conductivity-thickness product for 5-m intervals from the seafloor down to the depth where conductivity decreases to 1 S/m. We relate conductivities greater than 1 S/m to increasing amounts of conductive metal sulfides mixed with less conductive seawater-saturated fresh and altered basalts.

2.2. Bathymetry

The TAG hydrothermal field has been mapped with high-resolution (2 m; Figure 1) bathymetric surveys using an AUV-based multibeam echosounder. The SMS mounds have an almost circular base and a smooth to steep/rugged slope and confirm previous observations on lower-resolution data (White et al., 1998). Examples of these mounds are Shinkai, Southern, and Double mound (Figure 1) which are of conical shape. The MIR zone on the other hand has a more complex relief and a larger diameter. Inactive SMS mounds can be easily mistaken with volcanic mounds which consist mainly of basalt, although the latter have a more regular shape and have lower slope angles as is also the case at Endeavour Ridge (Jamieson et al., 2014).
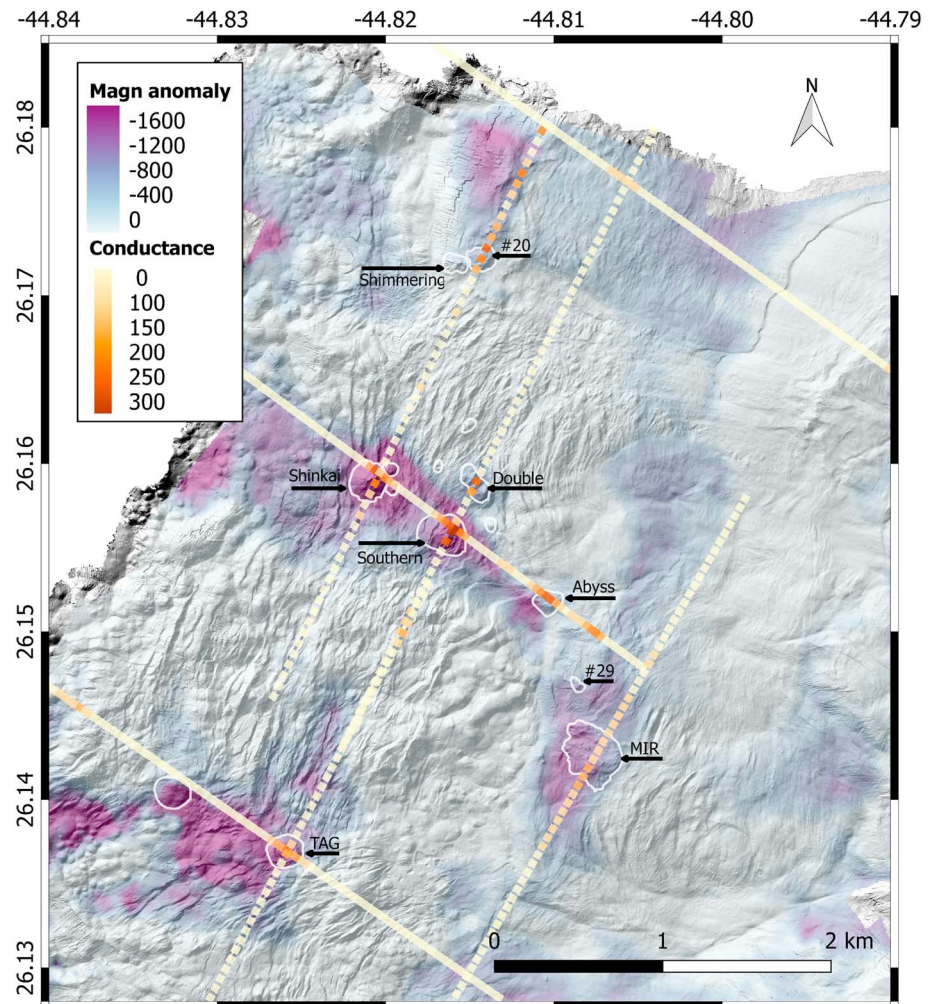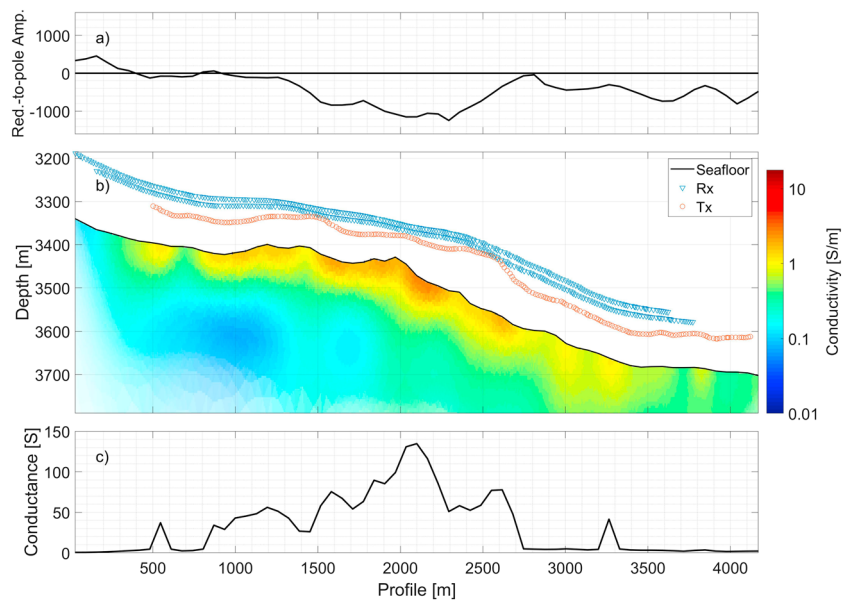
Figure 2. Reduced-to-the-pole magnetic anomaly map overlain by bathymetry hill shading, conductance for six profiles, and highlighted seafloor massive sulfide deposits identified from the bathymetry and verified with video footage or sampling. TAG = Trans-Atlantic Geotraverse.

2.3. Magnetics

The magnetic signature of the hydrothermal field (Szitkar & Dyment, 2015; Tivey et al., 1993, 1996) reveals a lack of magnetization below the active and inactive mounds which is likely caused either by alteration of the magnetic minerals of the upper crust during hydrothermal circulation and/or by the volume filled with nonmagnetic SMS deposits between the magnetometer and the oceanic crust (Szitkar et al., 2015). The magnetic data were recorded with the triaxial fluxgate sensor mounted on the AUV while flown at different altitudes between 20 and 100 m above the seafloor. Raw data were then adjusted for the effect of the vehicle magnetic signature, low-pass filtered and interpolated on a grid. Finally, magnetic anomalies were reduced-to-the-pole using the local inclination and declination of the geomagnetic field to place them above their causative sources within the crust.

2.4. Rock Physics

Rock samples were collected from TAG (SMS and jasper samples) either at outcrops on the seafloor by ROV HyBis or during subseafloor drilling (RD2; Lehrmann et al., 2018). These were supplemented by reference samples from outcrops on land (e.g., basalt from Cyprus). Samples where the electrical conductivity mechanism is dominated by ionic conduction in pore space (i.e., non-SMS samples) were measured with an ionic conductivity cell based on the device described by Zisser and Nover (2009). Because this configuration is susceptible to measurement artifacts caused by double layer polarization at any semiconductor (such as

Figure 3. (a) Reduced-to-the-pole magnetic anomaly interpolated from map shown in Figure 2. (b) The 2-D inversion results for controlled source electromagnetic profile across the MIR zone, overlain by data sensitivity, and positions of transmitter (circles) and receivers (triangles) in the water column. (c) Conductance estimated from panel (b) for conductivities above 1 S/m (yellow contour).

metal sulfides) to electrolyte interface (Stojek, 2010), the sulfide samples were measured using direct contact and/or inductive methods (Text S2).

3. Results

Inferred conductances are elevated for all known inactive deposits in the MIR and Alvin zone as well as the active TAG mound and coincide with negative reduced-to-the-pole magnetic anomalies (Figure 2). The observed CSEM data are fit well by the models (Figure S2), but biases remain, that are likely due to systematic errors such as the rough topography and the 3-D characteristics of the SMS target given the large footprint of the DASI-Vulcan array. A 2-D inversion of data from a conical 3-D structure may result in biases in the predicted versus observed data, and the inversion model may contain artifacts below and next to the mound structure, but the elevated conductivity within the mound can still be resolved adequately (Haroon et al., 2018).

3.1. MIR Zone

The MIR zone is located 4 km east off the Mid-Atlantic Ridge axis and covers a large area (∼1 km in diameter) with the only mound-like feature being <10 m high. Elevated heat flow values (Rona et al., 1996) indicate a late stage of hydrothermal activity. From the inferred final conductivity model for the North-South profile over the MIR zone (Figure 3b), a 50-m-thick, elongate, conductive anomaly is present immediately beneath the seafloor.

The magnetic profile across the MIR zone (Figure 3a) is interpolated from the reduced-to-the-pole magnetic map (Figure 2). A negative magnetic anomaly encompasses the maximum of the conductance (Figure 3c) along the profile. For most other SMS deposits, the highest conductances reside within the much larger areal extents of the magnetic anomalies that often connect adjacent deposits.

Although the CSEM method is sensitive to conductivity contrasts at the base of the sulfide deposit (Note: model cells with low data sensitivity are blanked out in Figure 3b), a strong conductivity contrast is not typically resolved because the sulfide content likely changes gradually with depth and because the inversion algorithm also favors smooth transitions.

3.2. Alvin Zone

The Alvin zone (Rona et al., 1993) encompasses the northern part of the hydrothermal field including Shinkai, Southern, Double, Rona, and Shimmering mound. Shinkai, target #20, Southern, Double, and the
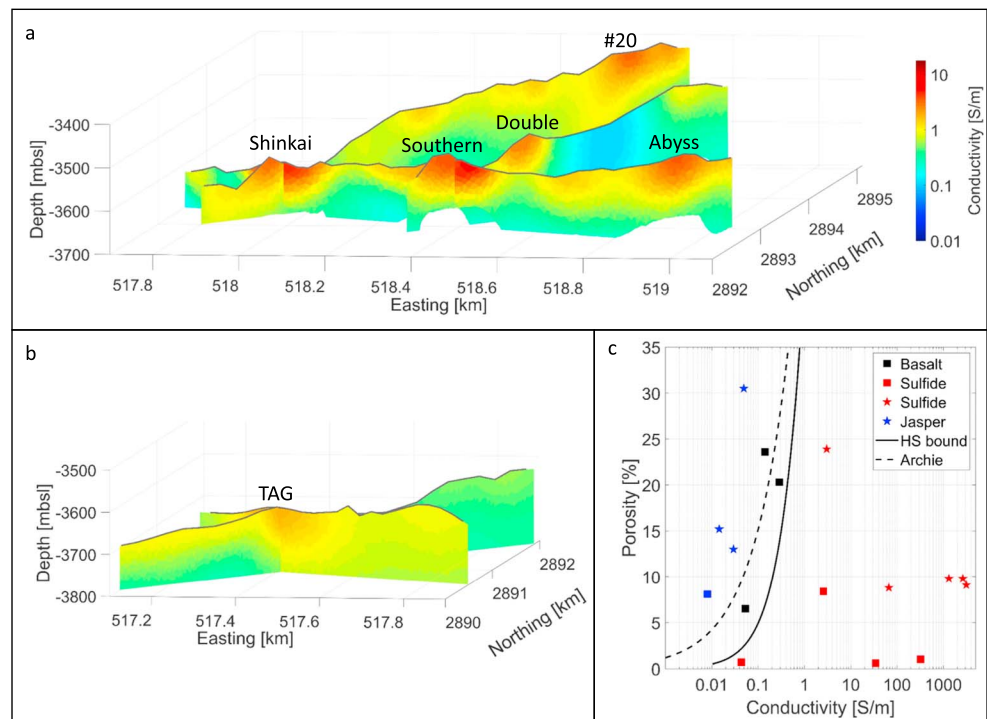
Figure 4. (a) Conductivity models across mounds Shinkai, Southern, Abyss, Double and target #20. (b) Conductivity models across TAG mound. (c) Porosity versus conductivity of selected samples from TAG (stars) and other sources (rectangles) for basalt (black), sulfide (red), and jasper (blue, a thin, <1-m, silicate-based layer above the sulfides; Lehrmann et al., 2018) samples; the Hashin Shtrikman upper bound (solid line) separates the main conduction mode via electrolytes (left) and metals/semiconductors (right), and the dashed line represents Archie's law approximation for electrolytic conduction in hard rock (Evans & Everett, 1994; Müller et al., 2018) with $a = 1$ and $m = 1.8$. TAG = Trans-Atlantic Geotraverse.

newly identified Abyss mound all exhibit distinct conductivity anomalies with conductivities up to 5 S/m (Figure 4a). The root of the mounds is expected to extend much deeper, but the denser silica-rich wall rock breccia and chloritized basalts tend to have much lower conductivities than the SMS deposits (Morgan, 2012). Seismic imaging of Shinkai and Southern mound also supports a deep reaching root (~220 m) consisting roughly of massive sulfide on top (approximately first 100 m) and a stockwork of brecciated sulfide, silica, and altered basalt underneath (Murton et al., 2019). The SMS deposit at Southern mound is inferred to be up to 80 m thick based on the CSEM data alone (Figure 4a) with an average conductivity of 3.7 S/m. A conductance of up to 300 S could also be translated in a thinner deposit of, for example, 60 m with an average conductivity of 5 S/m. Structures smaller than a few tens of meters are at the limit of resolution, so that a thin 10-m deposit of conductive material on top of the mound would appear as a thicker but less conductive cone top (Haroon et al., 2018). Southern mound has also been studied with the coincident loop system MARTEMIS, which is more downward looking and has a much smaller footprint than the towed CSEM system, and is more sensitive to conductive deposits with a higher vertical resolution but with a maximum penetration depth of about 50 m (Hölz & Jegen, 2016; Haroon et al., 2018). The 1-D inversion results of the MARTEMIS data reveal higher conductivities up to 10 S/m for the upper ~50 m below the mound's surface. Combining these observations suggests that the top of the deposit has a higher percentage of metal sulfides than the deeper sections.

The newly identified Abyss mound SMS occurrence was verified by video observations (Petersen and shipboard scientific party, 2016), and the presence of metalliferous sediments supports a past history of hydrothermal activity (Dutrieux et al., 2017). Geological and geochemical ground truthing therefore strengthens the interpretation based on bathymetry, CSEM, and magnetics. The area to the north of Shimmering mound (Figure 1) still shows some low-temperature hydrothermal activity (Rona et al., 1998) but was not sampled during our survey. A strong magnetic low and elevated conductivities, however, indicate

hydrothermal deposition around an unnamed mound (#7 in Humphris et al., 2015). Target #20 next to Shimmering mound also shows high conductivities seemingly belonging to the same hydrothermal system.

3.3. Active TAG Mound

The TAG mound is the only active mound in the TAG hydrothermal field. The negative magnetic anomaly extends west of TAG and coincides with other bathymetry-inferred targets. TAG mound has much lower inferred conductivities of up to 2 S/m than the inactive SMS mounds (Figure 4b). The active mound is different to the inactive mounds in three ways. The temperatures are distinctly higher (up to 360 °C) which could potentially increase the conductivities of the sulfides and pore fluids. On the other hand, it is anhydrite rich, which has a lower conductivity than sulfides, but dissolves at lower temperatures and is hence not present in the inactive mounds. The third difference is its smaller size (estimates of 2.7 million tonnes for TAG mound, Hannington et al., 1998, compared to up to 6.3 million tonnes for Southern mound, Murton et al., 2019). CSEM experiments in the 1990s at the TAG active mound with smaller transmitter-receiver spacings (<100 m) showed average conductivities (for homogeneous seafloor) of up to 16 S/m (Cairns et al., 1996), similar to the conductivities for a similar penetration depth of the MARTEMIS system at the inactive deposits (Haroon et al., 2018), suggesting that the lower inferred conductivities with the DASI-Vulcan system at the TAG mound are more likely caused by the target size compared to the transmitter-receiver spacing. The DASI-Vulcan system averages over a larger footprint and depth, and the adjacent altered basalt and increasing amount of silicate with depth likely impact the large-scale inferred conductivity compared to the short-offset, high-resolution methods. In fact, the geometry of the DASI-Vulcan array was chosen for fast, continuously towed, data collection over several kilometers with a wide footprint to detect SMS deposits large enough to be of economic interest.

3.4. Rock Physics

Conductivity measurements in the laboratory were made on five SMS samples collected on the seafloor by the ROV HyBis or recovered as core drilled by RD2 (Figure 1). The conductivities of SMS samples are up to 5 orders of magnitude higher than the reference basalt samples from outcrops on Cyprus, and although they have lower porosities (Figure 4c), they have the electrical conduction behavior characteristic of semiconductors/metals. By comparison, for the case of electrolytic conduction, the conductivity is directly related to the porosity of the sample (e.g., Archie's Law, Archie, 1942). This relationship does not hold for SMS deposits, which act as semiconductors causing the conductivities to be orders of magnitude higher and display complex behavior due to their frequency-dependent chargeability (Spagnoli et al., 2016, 2017). Samples from the Central Indian Ridge show similar behavior with a clear frequency dependence, for example, larger conductivities at higher frequencies (Müller et al., 2018). Here, the conductivities for the pure SMS samples are about 3 orders of magnitude larger than the conductivities inferred from the remote DASI-Vulcan array suggesting that the SMS deposits are locally richer and can be found at shallow depth below the surface but are likely mixed with silicates and altered basalts at greater depth. The results inferred from the DASI-Vulcan array average over the mound and cannot resolve features and structure at scales of less than a few tens of meters.

4. Discussion and Conclusions

We have presented how remote geophysical techniques have been successfully implemented to detect and localize SMS deposits in the TAG hydrothermal field. The deep-towed controlled source electromagnetic DASI-Vulcan experiment has been used to cover several kilometers long profiles with a lateral footprint of up to a few hundred meters across potential targets, some of which have been verified geologically before by localized sampling and video observations, while others were only recognized as potential targets from their shape (multibeam mapping). The CSEM data have confirmed known deposits and revealed previously uncertain ones. The inferred deposit thickness of up to 80 m is a maximum value as the inversion favors low conductivity gradients. Although the CSEM system is sensitive to the conductivity contrast between the pyrite-dominated SMS cap and the silicate-dominated stockwork, the product of thickness and conductivity can often be better resolved than individual parameters alone. Inferred conductivities reach up to 5 S/m, indicating the presence of semiconductors. The inferred values, however, are generally orders of magnitude lower than the conductivities of lab samples composed of pyrite with interconnected chalcopyrite. These lab samples were collected at the SMS deposits themselves and can reach conductivities of up to a few thousand Siemens per meter. The remotely inferred values are therefore average conductivities for volumes larger

than a few hundreds of cubic meters likely with decreased connectivity. Although the inferred conductivity structure is limited in resolution of a few tens of meters, the conductivity anomalies are generally localized to the deposit. In comparison, negative magnetic anomalies generally extend over larger areas than the deposit footprint because magnetic data are sensitive to the nonmagnetic SMS deposit itself and to the hydrothermally demagnetized stockwork and fault zones that surround and underlay the deposits at greater depth. High-resolution magnetics is therefore an indicator for where hydrothermal circulation was active on a larger scale. Sulfide deposits also have distinct surface expressions such as conical mounds and rough small-scale topography which can be interpreted with high-resolution bathymetry as long as the deposits are not overprinted with sedimentation or lava flows (camouflaged among volcanic, hummocky, mounds). Each of the geophysical methods alone provides a piece to the puzzle that evaluated individually may lead to ambiguous interpretations but together lead to a robust interpretations of the SMS potential.

In this work, we studied several inactive deposits up to ∼4 km from the ridge axis as well as the active TAG mound. TAG mound shows lower conductivities than seawater but is also smaller than most of the inactive deposits. Previous studies with a seafloor EM transmitter and receiver spacings of <100 m (Cairns et al., 1996) revealed higher conductivities (up to ∼16 S/m), similar to the conductivities for a similar penetration depth of the MARTEMIS system at the inactive deposits (Haroon et al., 2018) which suggests that the generally lower conductivities observed with the DASI-Vulcan system at TAG mound are probably related to the deeper penetration depth due to the larger transmitter-receiver spacing (350 and 505 m) and resulting averaging between highly conductive material just beneath the seafloor and less conductive stockwork material at greater depth. The smaller size of the TAG mound compared to the inactive deposits may in this case play a larger role than the possible effects of anhydrite (Lehrmann et al., 2018; Murton et al., 2019) and hot fluids (∼360 °C) which are only present in the active system.

To estimate the economic value of each deposit, it is essential to quantify the subseafloor geometry and probe the seafloor to understand the overall evolution of the deposit. Lander-type drilling shows that the content of valuable elements such as copper and zinc likely decreases with depth due to element remobilizing during the waning phase of hydrothermal activity (Lehrmann et al., 2018). The rich content of copper and zinc in surface samples and metalliferous sediments (Dutrieux et al., 2017) therefore does not represent the element concentration at depth. The elevated conductivities at greater depths might be caused by a large concentration of pyrite, which has no economic value (Murton et al., 2019). The deposit maximum thickness from CSEM extending beneath the base of the mounds on the seafloor supports the findings of Teagle and Alt (2004) that basaltic crust becomes heavily altered to secondary minerals such as silicates and chlorites with SMS inclusions.

We have shown that bathymetry, magnetic, and CSEM surveys are sensitive to different physical aspects of the deposits and therefore complement each other with a high success rate for detection and characterization of inactive deposits.

References

Archie, G. E. (1942). The electrical resistivity log as an aid in determining some reservoir characteristics. *Transactions of the American Institute of Mining, Metallurgical, and Petroleum Engineers*, *146*, 54–62.

Cairns, G. W., Evans, R. L., & Edwards, R. N. (1996). A time domain electromagnetic survey of the TAG hydrothermal mound. *Geophysical Research Letters*, *23*(23), 3455–3458. https://doi.org/10.1029/96GL03233

Constable, S. C., Kannberg, P. K., & Weitemeyer, K. (2016). Vulcan: A deep-towed CSEM receiver. *Geochemistry, Geophysics, Geosystems*, *17*, 1042–1064. https://doi.org/10.1002/2015GC006174

Constable, S. C., Parker, R. L., & Constable, C. G. (1987). Occam's inversion: A practical algorithm for generating smooth models from electromagnetic sounding data. *Geophysics*, *52*, 289–300.

Dutrieux, A., Lichtschlag, A., Murton, B. J., Petersen, S., Barriga, F., & Martins, S. (2017). *Metal mobilization in hydrothermal sediments*. Berlin, Germany: Paper presented at 49th Underwater Mining Conference.

Edwards, R. N. (1997). On the resource evaluation of marine gas hydrate deposits using sea-floor transient electric dipole-dipole methods. *Geophysics*, *62*(1), 63–74.

Edwards, R. N., & Chave, A. D. (1986). A transient electric dipole-dipole method for mapping the conductivity of the sea floor. *Geophysics*, *5*(4), 984–987.

Evans, R. L., & Everett, M. E. (1994). Discrimination of hydrothermal mound structures using transient electromagnetic methods. *Geophysical Research Letters*, *21*(6), 501–504. https://doi.org/10.1029/94GL00418

Gehrmann, R. A. S. (2019). Controlled-source electromagnetic data from the TAG hydrothermal field 26N Mid-Atlantic Ridge. PANGAEA. https://doi.pangaea.de/10.1594/PANGAEA.899073

Gehrmann, R. A. S., North, L. J., Lehrmann, B., & Murton, B. J. (2019). Rock physic samples from TAG, Mid-Atlantic Ridge, and various onshore samples. PANGAEA. https://doi.pangaea.de/10.1594/PANGAEA.899411

Hannington, M. D., Galley, A. G., Herzig, P. M., & Petersen, S. (1998). Comparison of the TAG mound and stockwork complex with Cyprus-type massive sulfide deposits. In *Proceedings-ocean drilling program scientific results* (Vol. 158, pp. 389–415).

Hannington, M. D., Jamieson, J., Monecke, T., Petersen, S., & Beaulieu, S. (2011). The abundance of seafloor massive sulfide deposits. *Geology*, *39*(12), 1155–1158. https://doi.org/10.1130/G32468.1

Haroon, A., Hölz, S., Gehrmann, R. A., Attias, E., Jegen, M., Minshull, T. A., & Murton, B. (2018). Marine dipole-dipole controlled source electromagnetic and coincident-loop transient electromagnetic experiments to detect seafloor massive sulfides: Effects of three-dimensional bathymetry. *Geophysical Journal International*, *215*(3), 2156–2171. https://doi.org/10.1093/gji/ggy398

Herzig, P. M., Humphris, S. E., Miller, D. J., & Zierenberg, R. A. (1998). Proceedings-ocean drilling program scientific results (Vol *158*). College Station, TX: Ocean Drilling Program. https://doi.org/10.2973/odp.proc.sr.158.1998

Hölz, S., & Jegen, M. (2016). How to find buried and inactive seafloor massive sulfides using transient EM-A case study from the Palinuro Seamount. Paper presented at EAGE/DGG Workshop on Deep Mineral Exploration, Münster, Germany.

Humphris, S. E., Herzig, P. M., Miller, D. J., Alt, J. C., Becker, K., Brown, D., & Zhao, X. (1995). The internal structure of an active sea-floor massive sulfide deposit. *Nature*, *377*, 713–716.

Humphris, S. E., Tivey, M. K., & Tivey, M. A. (2015). The Trans-Atlantic Geotraverse hydrothermal field: A hydrothermal system on an active detachment fault. *Deep Sea Research Part II: Topical Studies in Oceanography*, *121*, 8–16.

Jamieson, J., Clague, D., & Hannington, M. D. (2014). Hydrothermal sulfide accumulation along the Endeavour Segment, Juan de Fuca Ridge. *Earth and Planetary Science Letters*, *395*, 136–148.

Key, K. (2016). MARE2DEM: A 2-D inversion code for controlled-source electromagnetic and magnetotelluric data. *Geophysical Journal International*, *207*(1), 571–588.

Lalou, C., Reyss, J. L., Brichet, E., Rona, P. A., & Thompson, G. (1995). Hydrothermal activity on a 105-year scale at a slow-spreading ridge, TAG hydrothermal field, Mid-Atlantic Ridge (26°08′ N). *Journal of Geophysical Research*, *100*(B9), 17,855–17,862.

Lehrmann, B., Stobbs, I., Lusty, P., & Murton, B. J. (2018). Insights into extinct seafloor massive sulfide mounds at the TAG, Mid-Atlantic Ridge. *Minerals*, *8*(7), 302.

Morgan, L. A. (2012). Geophysical characteristics of volcanogenic massive sulfide deposits. *Volcanogenic Massive Sulfide Occurrence Model. US Geological Survey, Reston, VA*, *115*, 131.

Müller, H., Schwalenberg, K., Reeck, K., Barckhausen, U., Schwarz-Schampera, U., Hilgenfeldt, C., & von Dobeneck, T. (2018). Mapping seafloor massive sulfides with the Golden Eye frequency-domain EM profiler. *First Break*, *36*(11), 61–67.

Murton, B. J., Lehrmann, B., Dutrieux, A. M., Martins, S., de la Iglesia, A. G., Stobbs, I. J., et al. (2019). Geological fate of seafloor massive sulphides at the TAG hydrothermal field (Mid-Atlantic Ridge). *Ore Geology Review*, *107*, 903–925.

Myer, D., Constable, S., & Key, K. (2011). Broad-band waveforms and robust processing for marine CSEM surveys. *Geophysical Journal International*, *184*, 689–698.

Petersen, S. (2019). Bathymetric data products from AUV dives during METEOR cruise M127. PANGAEA. https://doi.pangaea.de/10.1594/PANGAEA.899415

Petersen, S., and shipboard scientific party (2016). Cruise report RV Meteor M127 - Metal fluxes and Resource Potential at the Slow-spreading TAG Midocean Ridge Segment (26° N, MAR) – Blue Mining@Sea. GEOMAR Report No.32. https://10.3289/GEOMAR_REP_NS_32_2016

Rona, P. A. (2003). Resources of the sea floor. *Science*, *299*(5607), 673–674.

Rona, P. A., Fujioka, K., Ishihara, T., Chiba, H., Masuda-Nakaya, H., Oomori, T., & Lalou, C. (1998). An active, low temperature hydrothermal mound and a large inactive sulfide mound found in the TAG hydrothermal field, Mid-Atlantic Ridge 26N, 45W. *EOS*, *79*, F920.

Rona, P. A., Hannington, M. D., Raman, C. V., Thompson, G., Tivey, M. K., Humphris, S. E., & Petersen, S. (1993). Active and relict sea-floor hydrothermal mineralization at the TAG hydrothermal field, Mid-Atlantic Ridge. *Economic Geology*, *88*(8), 1989–2017.

Rona, P. A., Petersen, S., Becker, K., Von Herzen, R. P., Hannington, M. D., Herzig, P. M., & Thompson, G. (1996). Heat flow and mineralogy of TAG relict high-temperature hydrothermal zones: Mid-Atlantic Ridge 26° N, 45° W. *Geophysical Research Letters*, *23*(23), 3507–3510.

Sinha, M., Patel, P., Unsworth, M., Owen, T., & MacCormack, M. (1990). An active source electromagnetic sounding system for marine use. *Marine Geophysical Researches*, *12*(1-2), 59–68.

Spagnoli, G., Hannington, M. D., Bairlein, K., Hördt, A., Jegen, M., Petersen, S., & Laurila, T. (2016). Electrical properties of seafloor massive sulfides. *Geo-Marine Letters*, *36*(3), 235–245.

Spagnoli, G., Weymer, B. A., Jegen, M., Spangenberg, E., & Petersen, S. (2017). P-wave velocity measurements for preliminary assessments of the mineralization in seafloor massive sulfide mini-cores during drilling operations. *Engineering Geology*, *226*, 316–325.

Stojek, Z. (2010). The electrical double layer and its structure. In F. Scholz et al. (Eds.), *Electroanalytical methods* (pp. 3–9). Berlin, Heidelberg: Springer.

Szitkar, F., & Dyment, J. (2015). Near-seafloor magnetics reveal tectonic rotation and deep structure at the TAG (Trans-Atlantic Geotraverse) hydrothermal site (Mid-Atlantic Ridge, 26 N). *Geology*, *43*(1), 87–90.

Szitkar, F., Petersen, S., Caratori Tontini, F., & Cocchi, L. (2015). High-resolution magnetics reveal the deep structure of a volcanic-arc-related basalt-hosted hydrothermal site (Palinuro, Tyrrhenian Sea). *Geochemistry, Geophysics, Geosystems*, *16*, 1950–1961. https://doi.org/10.1002/2015GC005769

Teagle, D. A., & Alt, J. C. (2004). Hydrothermal alteration of basalts beneath the Bent Hill massive sulfide deposit, Middle Valley, Juan de Fuca Ridge. *Economic Geology*, *99*(3), 561–584.

Tivey, M. A., Rona, P. A., & Kleinrock, M. C. (1996). Reduced crustal magnetization beneath relict hydrothermal mounds: TAG hydrothermal field, Mid-Atlantic Ridge, 26° N. *Geophysical Research Letters*, *23*, 3511–3514.

Tivey, M. A., Rona, P. A., & Schouten, H. (1993). Reduced crustal magnetization beneath the active sulfide mound, TAG hydrothermal field, Mid-Atlantic Ridge at 26 N. *Earth and Planetary Science Letters*, *115*(1-4), 101–115.

White, S. N., Humphris, S. E., & Kleinrock, M. C. (1998). New observations on the distribution of past and present hydrothermal activity in the TAG area of the Mid-Atlantic Ridge (26°08′ N). *Marine Geophysical Researches*, *20*(1), 41–56. https://doi.org/10.1023/A:1004376229719

Zisser, N., & Nover, G. (2009). Anisotropy of permeability and complex resistivity of tight sandstones subjected to hydrostatic pressure. *Journal of Applied Geophysics*, *68*(3), 356–370.